

Supplementary Information

A Novel Electroless Method for the Deposition of Single-Crystalline Platinum Nanoparticle Films On
an Organic Solid Matrix in the Presence of Gold Single Crystals

Khaleda Banu,[†], ^{‡,*} and Takayoshi Shimura[§]

[†]Department of Electrical & Computer Engineering, University of California, San Diego,
9500 Gilman Drive, La Jolla, San Diego, CA 92093-0407

[‡]Venture Business Laboratory, Center for Advanced Science and Innovation, Osaka University, Suita,
Osaka 565-0871, Japan

[§]Department of Material & Life Science, Division of Advanced Science and Biotechnology, Graduate
School of Engineering, Osaka University, Japan

*Corresponding author's E-mail: kbanu@ece.ucsd.edu, kbanu05@yahoo.com

Phone: +1-858-822-4629

1.1 Scheme for the deposition of Pt-NPs on the Au-SM

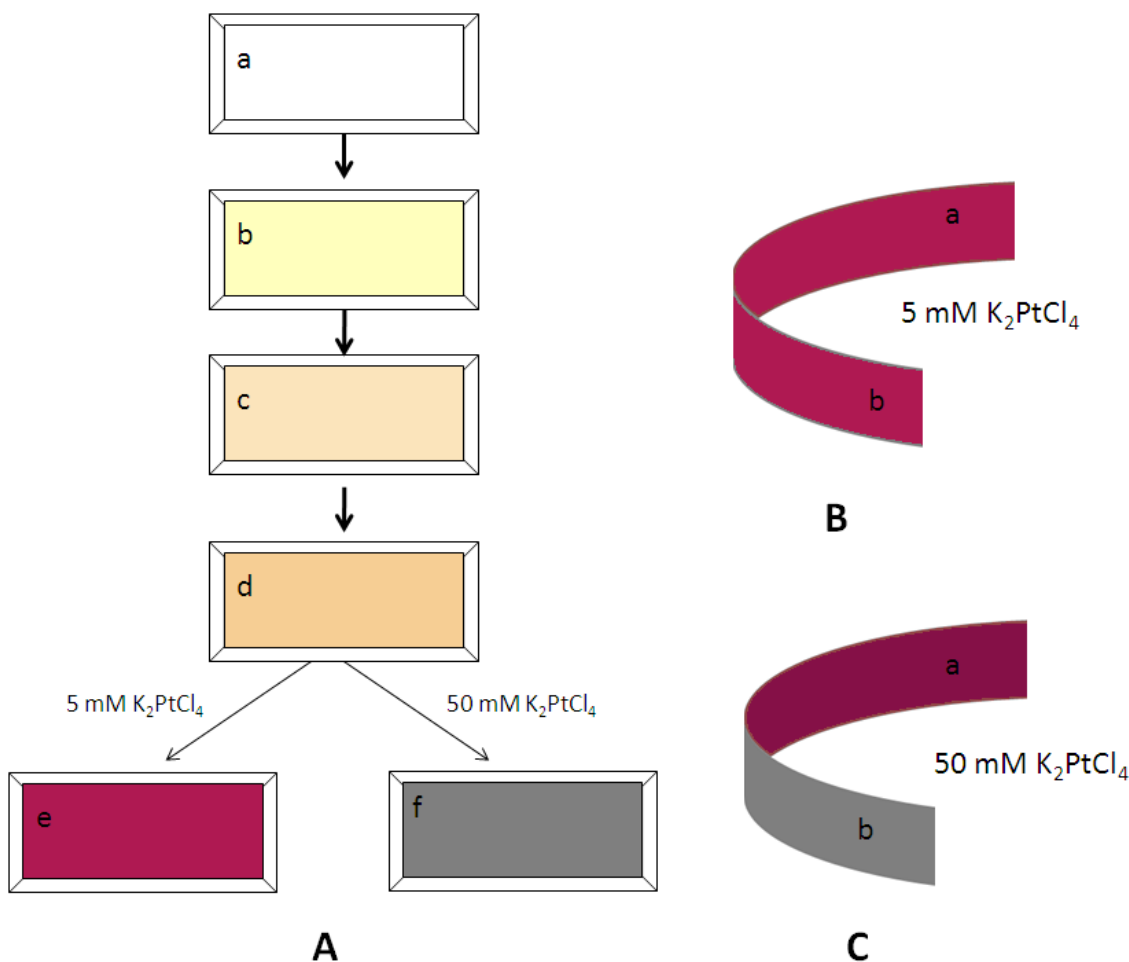


Fig. S1 (A) (a) Clean glass surface, (b) epoxy-thiol coated glass substrate, (c) tannin-immobilized epoxy-thiol-coated solid matrix, SM, (d) deposition of gold nanoparticles on the SM for 2 h, Au-SM, and (e and f) deposition of Pt-NPs on and inside the Au-SM when the concentration of K_2PtCl_4 in the aqueous phase is 5 mM (e) and 50 mM (f).

(B and C) Pictorial representations of the Pt-NPs deposited on solid matrices separated from the glass substrate in A(e) and A(f). Side (a) was attached to the glass surface and was not in contact with the solution during the reaction period. Side (b) was always in contact with the solution during the period of the reaction.

(B) Solid matrix from A(e) separated from the substrate after the Pt-NP deposition. The deep, ruby-red color of the Au-SM was observed on both the opposite side (a) and the solution side (b).

(C) The solid matrix from A(f) after the Pt-NP deposition. The deep ruby-red coloration of the SM observed from the opposite side (a) and the silver-grey coating observed from the solution side (b).

1.2 Simple experimental technique for the deposition of Pt-NPs on and inside the Au-SM

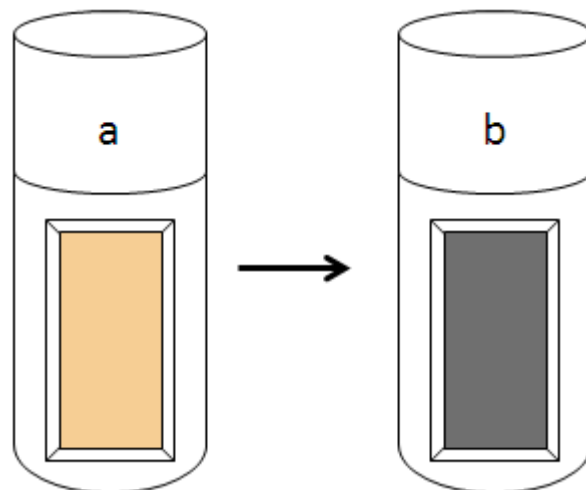


Fig. S2 (a) Insertion of Au-SM in 50 mM K_2PtCl_4 at 80 °C and a pH 1. (b) Formation of silver-grey coating of the Pt-NPs on the Au-SM after 24 h of heating.

1.3 Single-crystalline nature of Au-NPs deposited on the SM

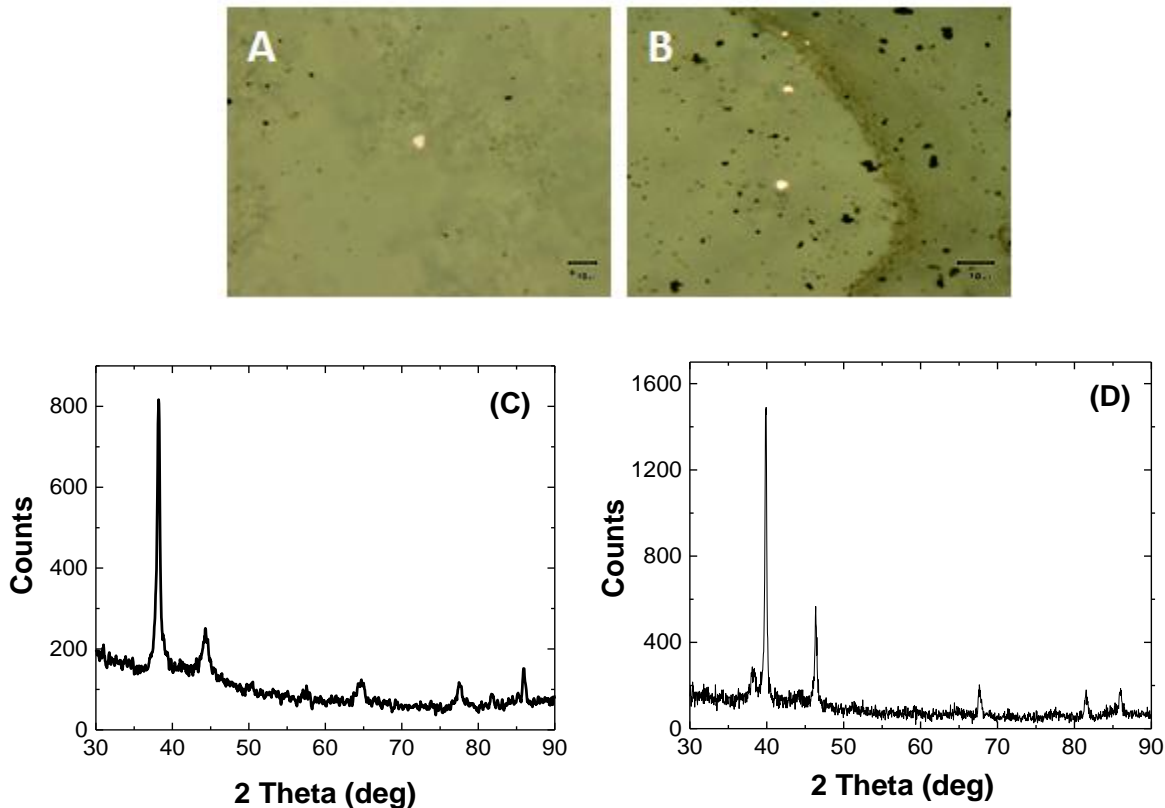


Fig. S3 (A and B) Optical microscopic images of the deposited gold particles on the SM for 2 h. A few gold nanosheets are clearly visualized by the optical microscopic measurement. (C) The XRD pattern of deposited Au-NPs on the SM (from A and B). This observation confirms that the deposited Au-NPs on the Au-SM was highly crystalline and anisotropic in nature and confined mainly by the $\{111\}$ planes. (D) The XRD pattern of the remaining Pt-NPs on the Au-SM after the silver-grey coating was detached from the surface. The solid matrix was washed several times before the measurement. One weak reflection at 38.2 indicates the presence of Au $\{111\}$ on the solid matrix. The intensity of the reflection from Au $\{111\}$ was decreased in (D) compared to the same reflection in (C).

1.4 Distribution of adsorbed Pt species on the solid matrices

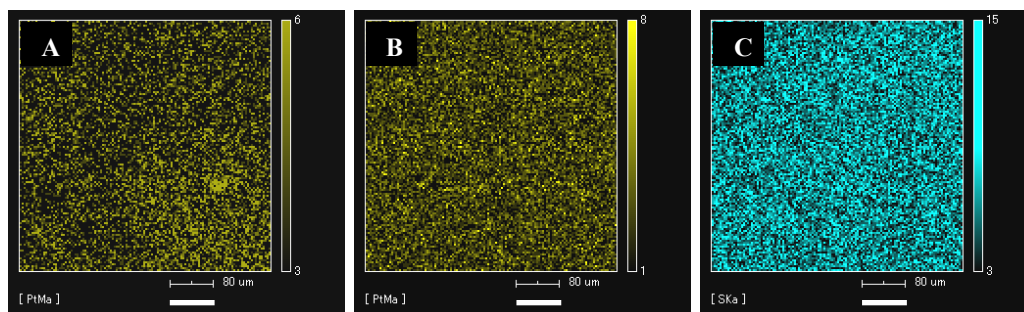


Fig. S4 EDX elemental maps of platinum species adsorbed on the epoxy-thiol coated solid matrix (A) and on the SM (B). Here, the concentration of K_2PtCl_4 in the solution phase was 5 mM, and the reaction was continued for 24 h. Elemental map of sulfur on the SM (C). The scale bar in A, B and C is equivalent to 80 μm .

1.5 Presence of metallic gold on the Au-SM after the Pt-NPs deposition

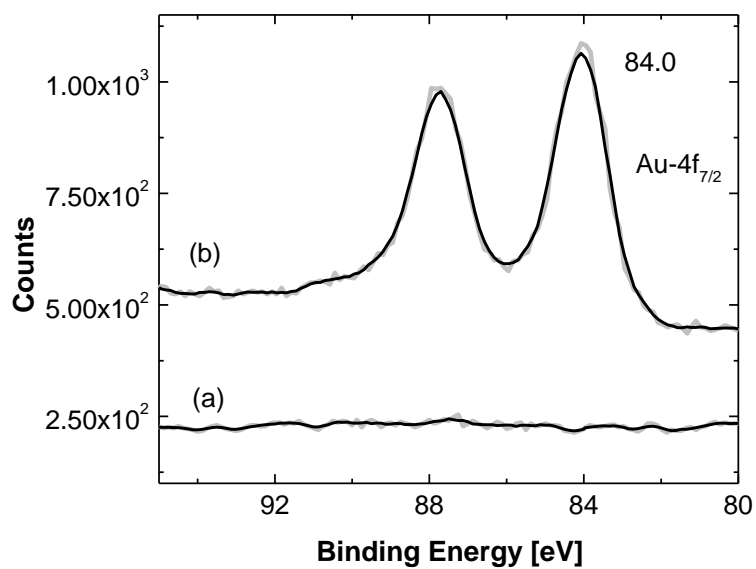


Fig. S5 The X-ray photoelectron spectra of the Au 4f region of the gold nanoparticles present on Au-SM after the deposition of Pt-NPs for a 5 mM K_2PtCl_4 in the solution phase. The data were obtained before (a) and after (b) the Ar^+ sputter-etching process. The peak position of Au 4f_{7/2} at 84.0 eV indicates the presence of Au^0 on the Au-SM.

1.6 Oxidation of Au-SM after the deposition of Pt-NPs

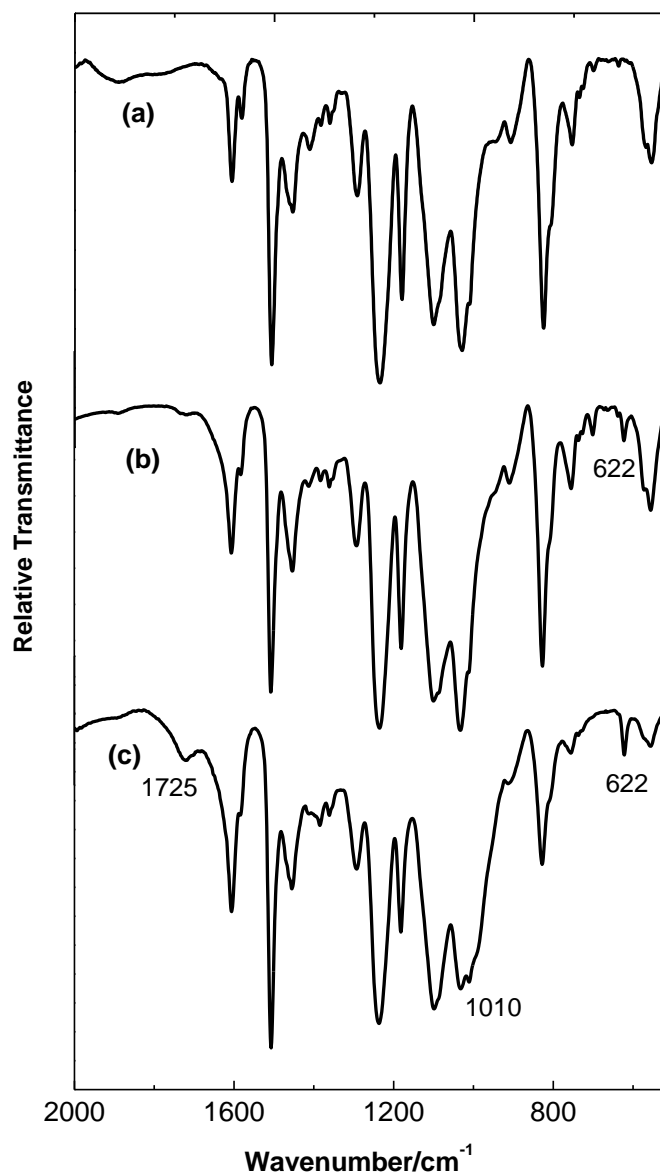


Fig. S6 FTIR-ATR spectra of the solid matrices after inserting in 5 mM K₂PtCl₄ for 24 h at 80 °C: (a) epoxy-thiol-coated glass substrate, (b) tannin immobilized epoxy-thiol-coated glass substrate, and (c) Au-SM.

The Pt-NPs were deposited on and inside the Au-SM as a result of interfacial redox reaction. The electron transfer from solid to liquid was coupled with the proton transfer from solid to liquid. The oxidation of the solid matrix was supported by the FTIR-ATR measurements. Characteristic peaks for

the oxidation of thiol derivatives and tannin appeared in FTIR-ATR measurements. The reaction between K_2PtCl_4 and thiol was initiated in the presence of minute Au-SCs. As the deposition of Pt begins, it can further act as a catalyst between the reaction of the remaining K_2PtCl_4 and the reducing agents in the solid matrix.

It is reported that ClO_4^- has characteristic absorption bands in the IR spectrum with peaks at $\sim 460\text{ cm}^{-1}$, 630 cm^{-1} , 932 cm^{-1} and 1115 cm^{-1} .^{1,2} In the present case, no band was observed at 460 cm^{-1} , but a characteristic absorption was observed at $\sim 622\text{ cm}^{-1}$ which was due to the formation of the thiirane ring of the sulfur compound. This result support that ClO_4^- was not adsorbed on the Au-SM.

The FTIR spectra for (a) and (b) is almost identical. However, in case of (b) a peak around 622 cm^{-1} was observed after the adsorption process. No characteristic peak for tannin oxidation was observed as supported by the absence of peak around 1725 cm^{-1} . Three new absorption bands with peaks at 622 cm^{-1} , 1010 cm^{-1} and 1725 cm^{-1} were observed after the reduction of K_2PtCl_4 to metallic platinum on and inside the Au-SM (c). The peak at 1725 cm^{-1} confirmed the presence of carbonyl functional groups on the SM because of the reduction of the hydroxyl groups of tannin molecules on the solid matrix. Here, the oxidation of tannin was due to the initial oxidation by $HAuCl_4$. However, the peaks at 622 cm^{-1} and 1010 cm^{-1} are associated with the oxidation of thiol derivatives on the SM. The peak at 622 cm^{-1} is due to the ring vibration of the thiirane compound generated after the reduction of $HAuCl_4$ and K_2PtCl_4 to the metallic state. The peak at 1010 cm^{-1} is due to the vibration of sulfoxyl (S=O) groups generated on the SM by the oxidation of thiol derivatives.

S7: Contribution of Au-NPs on the observed SPR absorption of Pt-NPs in the visible range

For the preparation of Au-SM, gold deposition was carried out at pH 1 with a 5 mM HAuCl_4 in the solution phase. The SM surface turned to pale brown after 2 h deposition. At this stage, the opposite side was not deep ruby-red in color. The size of the Au-NPs were estimated according to the so-called Scherrer formula from the broadening of different reflection peaks in the XRD spectrum as observed in Fig. S3. The estimated size along $\{111\}$ and $\{200\}$ planes were 21.3 nm and 9.4 nm, respectively. After the ruby-red Pt-NPs deposition, the size of Au-NPs along $\{111\}$ reflection was calculated as 15.4 nm from the XRD data as described in Fig 5B. The reflection from Au $\{200\}$ was very poor and was not considered for the size estimation. Here, on the top of the SM few larger Au-NSs were also present that was easily visualized by optical microscopic measurement. These particles may influence the size estimation as the contribution of larger crystals in XRD intensity is much pronounced over the small crystallites. Therefore, the actual size of the Au-NPs along $\{111\}$ orientation might be less than the calculated values.

The opposite side of the SM turned to deep ruby-red in color after 24 h of heating with a 5 mM HAuCl_4 . The surface of the SM (solution side) was never turned to ruby-red within 24 h. The reaction was very fast and all of the gold acid consumed within 24 h. The size of Au-NPs present on opposite side was calculated as 22.4 nm along the Au $\{111\}$ plane.³ On the opposite side of SM, no larger Au-NPs were present. Therefore, the size estimation from XRD peak broadening will be near to the actual value. The XPS signal for elemental gold was about two times more instance than the remaining gold on the SM after the Pt deposition as displayed in Fig S5 (compare S5 and Fig 5A in Ref. 3).

The whole SM turned to deep ruby-red in color when the concentration HAuCl_4 was 0.1 to 0.3 mM and reaction was continued for 24 h and 36 h, respectively.³ With this concentration ranges, the SM surface never turned to ruby-red within the 2 h of the synthesis process. The corresponding SPR absorption peaks were observed at 527 nm and 550 nm.³ This result support that transparent and ruby-red Au-NPs were deposited on the solution side of the SM surface as a result of slow reaction rate with a

0.1 to 0.3 mM HAuCl₄. When the deposition was carried out with 0.01 mM HAuCl₄, the SM turned to pale brown and was not turned to ruby-red even after heating for 24 h or more. This result indicates the absence of SPR absorption which might be due to the very small size (less than 2 nm) of the deposited Au-NPs on and inside the SM.⁴

The Au-SM turned to deep ruby-red in color within 2 h of synthesis when Pt deposition was started with 50 mM K₂PtCl₄ solution. For a 5 mM concentration, the Au-SM turned to ruby-red after 24 h. However, the intensity of XPS peak for Pt 4f was only 1.5 times more instance than the intensity of Au 4f (compare Fig. 6A and Fig. S5). This result indicates that the deposition of Pt was much slower than the deposition of Au. Here the Pt and Au deposition was continuing for 24 h and 2 h, respectively.

From the experimental finding it was clear that the Au-SM surface became ruby-red within 2 h of Pt deposition. The Pt deposition was a slower process than the Au deposition. For gold deposition the SM turned to ruby-red after 36 h to 48 h. This result support that most probably the absorption co-efficient of Pt-NPs is much higher than that of the Au-NPs.

The diffusion of Au atoms through the SM was possible during the deposition of Pt-NPs. This was supported by the fact that the size of Au-NP along Au{111} was decreased from 21.3 nm to 15.4 nm after the Pt-NPs deposition. The decrease of XRD signal from Au{111} and other reflections also supported the diffusion of Au through the SM. The Au-NPs on and inside the SM was charge neutral and was not experienced by any partial positive charge.³

From the above results it can be conclude that the ruby-red color of the Au-SM after the Pt-NPs deposition was purely due to the SPR absorption of Pt-NPs. However, some contribution may arise from the Au-NPs formed inside the SM as a result of atomic gold diffusion during the deposition process.³ Further investigation is necessary to clarify any contribution of Au-NPs on the SPR absorption of PT-NPs deposited on and inside the Au-SM.

References

- 1 H-W. Chen, C-H. Jiang, H-D. Wu, F-C. Chang, *J. Appl. Polym. Sci.* 2004, **91**, 1207.
- 2 Y. Chen, Y-H. Zhang and L-J. Zhao, *J. Appl. Polym. Sci.*, 2004, **91**, 1207.
- 3 K. Banu and T. Shimura, *New J. Chem.*, 2011, **35**, 1031.
- 4 S. Link, M. A. El-Sayed. *Annu. Rev. Phys. Chem.*, 2003, **54**, 331.